

# Terahertz pulse generation in an organic crystal by optical rectification and resonant excitation of molecular charge transfer

John J. Carey

*Department of Physics, University of Strathclyde, Glasgow, Scotland*

Ray T. Bailey, D. Pugh, J. N. Sherwood, and F. R. Cruickshank

*Department of Pure and Applied Chemistry, University of Strathclyde, Glasgow G4 0NG, Scotland*

Klaas Wynne<sup>a)</sup>

*Department of Physics, University of Strathclyde, Glasgow, Scotland*

(Received 18 July 2002; accepted 11 October 2002)

Organic molecular crystals that are extremely efficient at terahertz-pulse generation are investigated. Terahertz pulses produced by optical rectification at 800 nm in (–)2-( $\alpha$ -methylbenzyl-amino)-5-nitropyridine have an order of magnitude higher power than those generated in the commonly used inorganic crystal ZnTe. The organic molecular crystals were also found to generate terahertz pulses when excited on resonance at 400 nm. This may pave the way for studying ultrafast charge-transport dynamics in three dimensions. © 2002 American Institute of Physics. [DOI: 10.1063/1.1527237]

The generation, detection, and application of subpicosecond pulses in the terahertz (THz) region of the spectrum are currently of considerable interest. THz pulses have been used in a wide range of experiments from simple spectroscopy and time-resolved pump-probe experiments to imaging applications. There are a number of different techniques available for the generation and detection and the decision on which to use for an experiment will generally be based upon whether high power or broad spectral bandwidth is required. High electric-field strengths can be obtained from large-area dc-biased photoconductive antennas.<sup>1</sup> However, this method generally limits the bandwidth to a few THz and can produce unwanted rf noise. Optical rectification with nonlinear crystals<sup>2</sup> is therefore a common choice for THz experiments as this produces high signal-to-noise ratios and a very broad bandwidth. ZnTe is currently the most popular choice for optical rectification as it can be used to generate extremely short and high-quality THz pulses<sup>3</sup> and can also be used for detection via electro-optic sampling (EOS).

Organic crystals such as DAST<sup>4</sup> have been a recent source of interest as they have been reported to generate stronger fields than ZnTe when used for optical rectification. However, the THz fields generated by crystals such as DAST and, more recently, N-benzyl-MNA (Ref. 5) are more complicated in both the time and frequency domain. Phonon bands in the crystals result in the production of a smaller range of frequencies than ZnTe.<sup>5</sup> Crystals such as DAST also have a large birefringence complicating their application.<sup>4</sup> This has resulted in ZnTe remaining the THz generator of choice.

We have investigated a range of organic molecular crystals and found that the crystal (–)2-( $\alpha$ -methylbenzyl-amino)-5-nitropyridine (MBANP)<sup>6</sup> is superior to ZnTe when used for optical rectification at 800 nm. In addition, this crystal generates THz radiation when

excited on resonance at 400 nm, opening up a revolutionary way of measuring the transport of charge.<sup>7,8</sup> MBANP generates optically rectified THz pulses that are similar temporally and spectrally to those generated by ZnTe. MBANP has the added advantage of being relatively easy to grow in single crystals probably due to its L-shaped structure and strong H bonding in certain directions as well as a suitable habit. Crystals as large as  $10 \times 7 \times 7$  cm<sup>3</sup> have been grown in our labs.<sup>9</sup>

The configuration for generation and detection of THz pulses is shown in Fig. 1. The output from a 1 kHz regenerative amplifier producing 40-fs 1.2-mJ pulses at 800 nm was passed through a 95% reflecting beam splitter. The weaker transmitted portion was used as the gate (or probe) beam and the reflected as the pump (or excitation) beam. The pump beam was focused through the generating crystal where the beam diameter was approximately 8 mm. The generated THz radiation leaves the crystal with a curved wave front and is therefore already focusing. The focusing THz

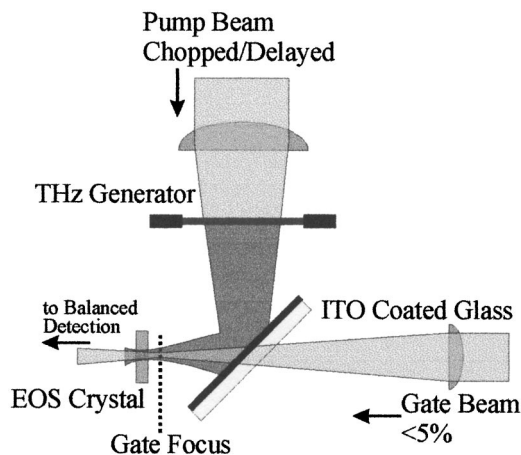


FIG. 1. Layout of the terahertz setup used in the experiments. Both the pump and the gate beams are initially *p* polarized. The EOS crystal was a 0.2 mm (110)-cut ZnTe crystal.

<sup>a)</sup>Electronic mail: klaas.wynne@physics.strath.ac.uk

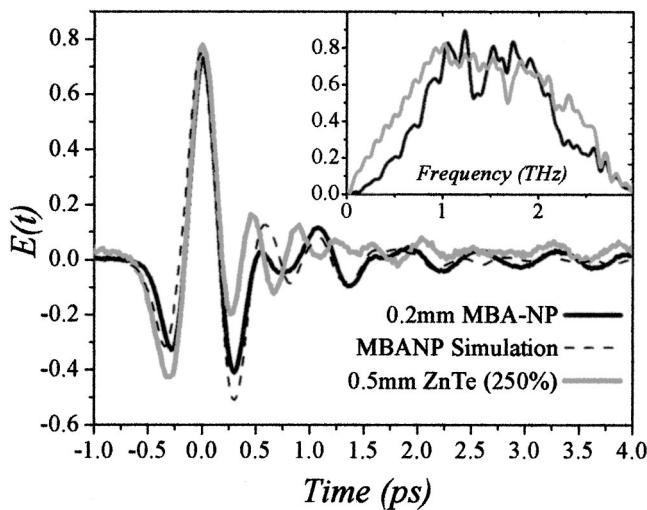


FIG. 2. Time-domain electric-field traces of optical rectification of 800 nm pulses in 0.2 mm MBANP and 0.5 mm ZnTe crystals. The simulated generation in MBANP and subsequent detection in ZnTe is also shown. The ZnTe curve has been scaled up by a factor of 2.5. (inset) Fourier spectra of the time-domain traces.

light reflects from an indium-tin-oxide (ITO) coated glass plate such that the focal point occurs in an EOS detection crystal. The ITO layer acts as a beam splitter, reflecting most of the THz pulse, and transmitting a large portion of the gate. This configuration allows for the detection of stronger signals without resorting to awkward THz focusing elements. The gate beam is focused by a 20 cm focal-length lens positioned so that the focal point occurs at a small distance in front of the detection crystal. Making the gate spot size in the crystal bigger in this manner increased the signal strength without changing the shape of the detected THz field. The THz pulse is then detected by standard EOS and balanced detection<sup>10</sup> using a 0.2 mm  $\langle 110 \rangle$ -cut ZnTe crystal mounted on a 0.5 mm  $\langle 100 \rangle$ -cut ZnTe crystal to prevent reflections.

The MBANP crystal is  $P2_1$  monoclinic<sup>6</sup> and the samples used were cleaved in the  $\langle 001 \rangle$  plane and illuminated along the  $\langle 001 \rangle$  axis. The 200  $\mu\text{m}$  MBANP crystals absorb all wavelengths below 450 nm and the crystal is excited with either 800 nm or 400 nm light for excitation on or off resonance. A half-wave plate and 200  $\mu\text{m}$  BBO crystal can be placed in the pump beam to excite the MBANP crystal on resonance. A Newport BG40 glass filter is then placed between the BBO and MBANP crystals to prevent the generation of a rectification signal by the fundamental frequency. A 0.5 mm  $\langle 110 \rangle$  ZnTe crystal was also used to generate via optical rectification for comparison. No laser damage was observed in either ZnTe or MBANP with the 800 nm pump beam (incident energies remained below  $10 \mu\text{J}/\text{cm}^2$ ). However, at 400-nm wavelengths, dark burn marks could be observed easily by the naked eye in MBANP when the energy of the 40-fs pump pulse was above  $0.1 \mu\text{J}/\text{cm}^2$ .

Optical rectification of 800 nm pulses in MBANP or ZnTe results in the THz pulses presented in Fig. 2. It can be seen that the signals are very similar in shape in both the frequency and time domain. However, MBANP produces a much stronger signal due to its larger electrooptic coefficient ( $r_{\text{eff}} = 18.2 \text{ pm V}^{-1}$  at 632.8 nm).<sup>11</sup> The group index at 800 nm of MBANP was measured in the  $\langle 001 \rangle$  plane along the

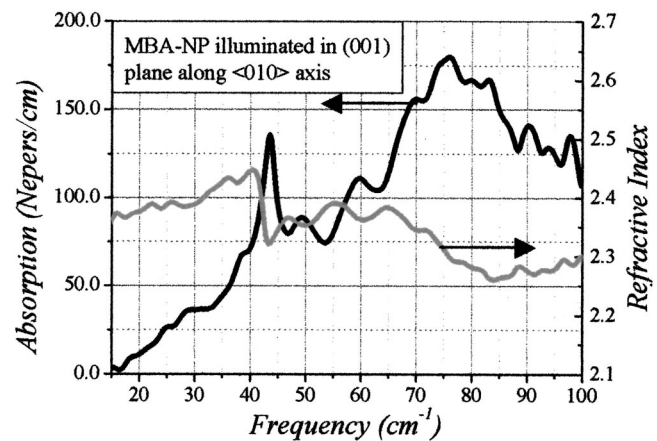


FIG. 3. The absorption and refractive index of  $\langle 001 \rangle$  MBANP at THz frequencies. Poor signal to noise prevents the acquisition of reliable data outside the 0.5–3.0 THz range.

$\langle 010 \rangle$  axis to be  $2.62 \pm 0.03$ . Figure 3 shows the refractive index and absorption coefficient at THz frequencies in MBANP. While MBANP is naturally birefringent, the optically rectified signal is always generated along the  $b$  axis. This means that the generated optical-rectification signal is always linearly polarized when excited along the  $\langle 001 \rangle$  axis. When exciting on resonance, the signal is generated by a direct intramolecular charge transfer<sup>12</sup> within the MBANP molecules. Figure 4 shows the signal detected when the MBANP molecules undergo excitation by 400 nm light polarized along the  $b$  axis. In this case, the two excited molecules in the unit cell will initially combine to produce a linearly polarized THz pulse. However, when excited at an angle to the  $b$  axis, the signal polarization will be changed by the birefringence of the crystal.

A number of other crystals similar to MBANP were studied in less detail. It was found that 4-(N,N-dimethylamino)-3-acetamidonitrobenzene (DAN) and 4-nitro-4'-methylbenzylidene aniline (NMBA) produce THz pulses through optical rectification of 800 nm pulses of comparable strength to MBANP. Like MBANP, NMBA is also relatively easy to grow, but DAN is much more difficult owing to its needlelike habit and obtainable crystal size is

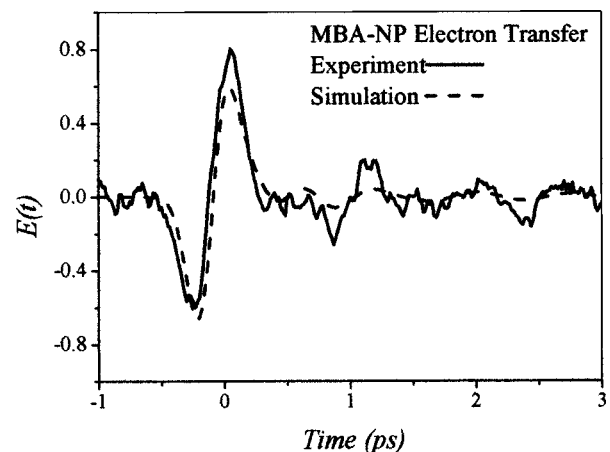


FIG. 4. THz signal generated from MBANP when excited on resonance by a 400 nm pulse. In this case, the THz field is generated by the polarization change that occurs when the MBANP molecules undergo direct electron transfer.

limited. However, phonon-band absorption limits their power in the 1.6 to 3 THz range.

Whether exciting on or off resonance, as the pump pulse propagates through a generation crystal it generates a nonlinear polarization wave traveling with the group velocity of the pump pulse. A theoretical model has been developed describing the THz field generated by such a polarization wave. The one-dimensional model assumes plane waves but otherwise makes no assumptions such as the slowly varying envelope or the rotating-wave approximation. In the far field, the generated THz field can be shown to be given by

$$\tilde{E}(L_1) = \frac{i\omega\tilde{G}\tilde{r}}{2\tilde{n}} \frac{e^{ikL_1\tilde{n}} - e^{ikn_{g,\text{vis}}L_1}}{n_{g,\text{vis}} - \tilde{n}}, \quad (1)$$

where  $\tilde{E}(L_1)$  is the Fourier transform of the generated THz pulse for a crystal of length  $L_1$ ,  $\tilde{r}$  is the appropriate frequency-domain response function of the THz generator,  $\tilde{G}$  is the intensity envelope of the pump pulse in the frequency domain, and  $n_{g,\text{vis}}$  is the group index of the pump pulse in the generation medium. The frequency-dependent complex refractive index for the generated THz pulse is given by  $\tilde{n}$ . Absorption of the pump pulse may also be included by making  $n_{g,\text{vis}}$  complex. Detection of the THz pulses through EOS can be calculated using<sup>13</sup>

$$\Delta I_{\text{EOS}}(\tau) \propto \int d\omega \tilde{G}\tilde{E}(L_1) e^{-i\omega\tau} \frac{e^{i\omega[\tilde{n} - n_{g,\text{vis}}]L_2/c} - 1}{i\omega[\tilde{n} - n_{g,\text{vis}}]/c}, \quad (2)$$

where  $\Delta I_{\text{EOS}}(\tau)$  is the EOS signal as a function of pump-gate delay  $\tau$  in a detection crystal of length  $L_2$ . In Eq. (2),  $\tilde{n}$  and  $n_{g,\text{vis}}$  now represent indices in the detection material, i.e., ZnTe. An analytical expression for the complex refractive index was determined by fitting the absorption spectra of ZnTe (Ref. 14) and MBANP to a multiple harmonic-oscillator model.

In the case of optical rectification, the response function  $\tilde{r}$  is set equal to the (frequency-dependent) electro-optic coefficient. When MBANP is excited on resonance (see Fig. 4), the signal is not from optical rectification but direct charge transfer.<sup>12</sup> In this case,  $\tilde{r}$  is equal to the frequency-dependent response function

$$\tilde{r} = \frac{3\tilde{\epsilon}}{2\tilde{\epsilon} + 1} \frac{N\Delta\mu}{\gamma - i\omega}, \quad (3)$$

where  $N$  is the number density of radiating dipoles,  $\Delta\mu$  is the change in the permanent dipole moment upon excitation,  $\gamma$  is the rate of thermal back electron transfer, and  $\tilde{\epsilon}$  is the frequency-dependent dielectric function ( $\tilde{n} = \sqrt{\tilde{\epsilon}}$ ). Numerical calculations based on this model are shown in Figs. 2 and 4.

The organic molecular crystals studied here can be used to optically rectify ultrashort 800 nm pulses and produce THz pulses of similar quality (temporally and spectrally) to those from ZnTe. The generated THz peak field strength in

MBANP is 2.5 times higher than in ZnTe for a shorter path-length. Using the theory described here, it can be shown that this corresponds to  $\sim 28$  times higher peak power when both crystals are 0.2 mm. The energy of the terahertz pulses generated by optical rectification in 0.2 mm of MBANP is estimated to be 3 nJ, corresponding to a conversion efficiency of  $10^{-4}$ . The organic molecular crystals studied here could be grown to large aperture sizes for high power applications. Such crystals would produce THz peak field strengths comparable to those from large-area dc-biased photoconductive antennas but with a much shorter pulse length, much broader bandwidth, and no rf noise.

The production of THz pulses by exciting the organic molecular crystals on resonance is due to electron transfer within the constituent molecules. By varying the crystal orientation, the polarization of the exciting light, and the detected polarization of the emitted THz field, it is possible to determine the absolute orientation in space of the current associated with the electron-transfer process. Therefore, this technique presents an interesting way to study the details of charge transport.

The authors gratefully acknowledge D. Jones, S. Jamison, and R. Issac for experimental support and EPSRC for financial support. Acknowledgement is also made to the donors of The Petroleum Research Fund, administered by the ACS for support of this research. The experiments were performed in the Strathclyde Electron and Terahertz to Optical Pulse Source (TOPS).<sup>15</sup>

- <sup>1</sup>E. Budiarto, N.-W. Pu, S. Jeong, and J. Bokor, *Opt. Lett.* **23**, 213 (1998).
- <sup>2</sup>X.-C. Zhang, X. F. Ma, Y. Jin, T.-M. Lu, E. P. Boden, P. D. Phelps, K. R. Stewart, and C. P. Yakymyshyn, *Appl. Phys. Lett.* **61**, 3080 (1992).
- <sup>3</sup>A. Leitenstorfer, S. Hunsche, J. Shah, M. C. Nuss, and W. H. Knox, *Appl. Phys. Lett.* **74**, 1516 (1999).
- <sup>4</sup>P. Y. Han, M. Tani, F. Pan, and X.-C. Zhang, *Opt. Lett.* **25**, 675 (2000).
- <sup>5</sup>H. Hashimoto, H. Takahashi, T. Yamada, K. Kuroyanagi, and T. Kobayashi, *J. Phys.: Condens. Matter* **13**, L529 (2001).
- <sup>6</sup>R. T. Bailey, G. Bourhill, F. R. Cruickshank, D. Pugh, J. N. Sherwood, G. S. Simpson, and S. Wilkie, *Mol. Cryst. Liq. Cryst.* **231**, 223 (1993).
- <sup>7</sup>A. Leitenstorfer, S. Hunsche, J. Shah, M. C. Nuss, and W. H. Knox, *Phys. Rev. B* **61**, 16642 (2000).
- <sup>8</sup>M. C. Beard, G. M. Turner, and C. A. Schmuttenmaer, *J. Phys. Chem. A* **106**, 878 (2002).
- <sup>9</sup>R. T. Bailey, F. R. Cruickshank, D. Pugh, and J. N. Sherwood, *Acta Crystallogr., Sect. A: Found. Crystallogr.* **47**, 145 (1991).
- <sup>10</sup>J. J. Carey, J. Zawadzka, D. A. Jaroszynski, and K. Wynne, *Phys. Rev. Lett.* **84**, 1431 (2000).
- <sup>11</sup>R. T. Bailey, G. H. Bourhill, F. R. Cruickshank, D. Pugh, J. N. Sherwood, G. S. Simpson, and K. B. R. Varma, *J. Appl. Phys.* **75**, 489 (1994).
- <sup>12</sup>K. Wynne and R. M. Hochstrasser, *Adv. Chem. Phys.* **107**, 263 (1999).
- <sup>13</sup>H. J. Bakker, G. C. Cho, H. Kurz, Q. Wu, and X. C. Zhang, *J. Opt. Soc. Am. B* **15**, 1795 (1998).
- <sup>14</sup>G. Gallot, J. Q. Zhang, R. W. McGowan, T. I. Jeon, and D. Grischkowsky, *Appl. Phys. Lett.* **74**, 3450 (1999).
- <sup>15</sup>D. A. Jaroszynski, B. Ersfeld, G. Giraud, S. Jamison, D. R. Jones, R. C. Issac, B. M. W. McNeil, A. D. R. Phelps, G. R. M. Robb, H. Sandison, G. Vieux, S. M. Wiggins, and K. Wynne, *Nucl. Instrum. Methods Phys. Res. A* **445**, 317 (2000).